Cell-Free Massive MIMO with Underlay Spectrum-Sharing

Diluka Loku Galappaththige and Gayan Amarasuriya
Department of Electrical and Computer Engineering, Southern Illinois University, Carbondale, IL, USA 62901
Email: {diluka.lg,gayan.baduge}@siu.edu

***Abstract*—In this paper, the coexistence of cell-free massive multiple-input multiple-output (MIMO) and underlay spectrum-sharing is investigated. Thereby, the fundamental performance limits are established to characterize the feasibility of this coexistence. A set of spatially-distributed secondary access points (S-APs), which are underlaid in a primary cell-free massive MIMO system, serves many secondary users (SUs) in the same licensed spectrum of the primary access points (P-APs). Stringent secondary transmit power constraints are defined for the S-APs to mitigate undesired secondary co-channel interference (CCI) at the primary users (PUs). The uplink channels are estimated locally at the P-APs and S-APs via a generalized pilot sharing scheme, and thereby, conjugate precoders are used to serve PUs/SUs simultaneously. The achievable rates for both primary and secondary systems are derived for imperfectly estimated channels at the P-APs/S-APs, and the impact of intra-system pilot contamination is investigated. User-fairness for SUs is guaranteed by designing an efficient transmit power control policy based on the max-min criterion and secondary transmit power constraints. Through a rigorous analysis, we reveal that massive distributed primary/secondary transmissions can be exploited to mitigate detrimental impact of secondary CCI on PUs, and thereby, the achievable rates of primary/secondary systems can be boosted.**

I. Introduction

Massive multiple-input multiple-output (MIMO) systems operating in sub-6 GHz bands have been recognized as one of the key enabling technologies for the next-generation wireless standards [1]. By virtue of massive antenna arrays at the base-stations (BSs), many distributed user nodes can be served simultaneously in the same time-frequency resource block by spatial-domain multiplexing. Recently, a cell-free version of massive MIMO in which a large number of spatially-distributed access points (APs) is employed to provide a uniform service to user nodes within a much larger geographical area has gained research attention [2]–[5]. Cell-free massive MIMO aims to boost the achievable rates by circumventing the impediments due to spatially-correlated fading at BS antenna arrays, shadowing due to large obstacles and effectively reducing the end-to-end transmission distances between APs and users [3]–[5].

Spectrum underutilization/holes can be effectively combated via spectrum-sharing techniques [6]. Specifically, in underlay spectrum-sharing, a secondary system can be underlaid within a primary system having a licensed primary spectrum, and thereby, overall spectrum efficiency can be significantly boosted [6]. An underlaid secondary system can be thus operated in the same licensed primary spectrum by carefully defining the secondary transmit power constraints such that the secondary co-channel interference (CCI) inflicted at the primary receivers always falls below a predefined interference threshold (PIT). This PIT is the maximum allowable CCI for the primary system to operate with no/limited performance degradation [6].

The coexistence of underlay spectrum-sharing and massive MIMO with co-located antenna arrays has already been explored [7]–[11]. An initial foundation for exploring the feasibility of underlay spectrum-sharing in massive MIMO systems has been established in [7]. The impact of inherent intra/inter-cell pilot contamination in multi-cell multi-user massive MIMO systems with spectrum-sharing has been quantified in [8]. The achievable rates of dual-hop enabled massive MIMO spectrum-sharing systems have been derived in [9]. Reference [10], relay selection strategies for massive MIMO two-way relaying have been explored by quantifying fundamental performance limits. In [12], performance bounds of spectrum-sharing in massive MIMO systems with stochastic BS and user locations have been derived.

A key attribute to all aforementioned related prior research on the coexistence of massive MIMO and underlay spectrum-sharing is that the antenna arrays at the BSs are co-located. To the best of our knowledge, this coexistence and underlying performance limits in a cell-free massive MIMO setting have not yet been investigated. Thus, the underlying performance metrics can be hindered by spatial correlation at massive antenna arrays and shadow fading due to large obstacles. As a remedy, in this paper, we explore the practical viability of the coexistence of cell-free massive MIMO with underlay spectrum-sharing. Moreover, the distributed transmissions may be beneficial in an underlay spectrum-sharing set-up by effectively reducing the end-to-end secondary transmission distances and thereby minimizing the secondary CCI inflicted at the primary receivers. Moreover, since there are no cell boundaries and users are much closer to APs in a cell-free setting, the primary/secondary systems can offer a high coverage area with high coverage probability. Thereby, the achievable rates of both systems may be boosted significantly. Aiming at exploring the joint benefits, we investigate the fundamental performance limits of underlay spectrum-sharing in a cell-free massive MIMO setting.

Our contribution: The feasibility of the coexistence of time-division duplex (TDD) based cell-free massive MIMO and underlay spectrum-sharing is investigated by establishing the fundamental performance limits. To this end, a secondary system with distributed secondary access points (S-APs) is underlaid within a primary system based on a cell-free massive MIMO set-up. The uplink channels are locally estimated at the primary access points (P-APs) and S-APs by using pilots sent by primary users (PUs)/ secondary users (SUs) based on a generalized pilot sharing scheme in order to minimize the training overhead. Then, the spatially-distributed PUs and

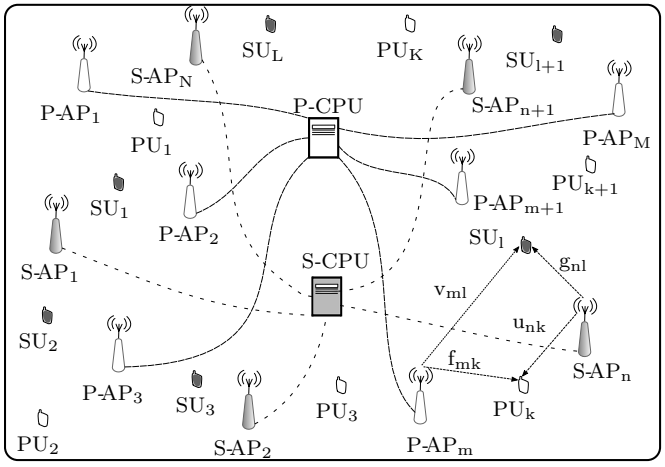

Fig. 1. A cell-free massive MIMO system with underlay spectrum-sharing.

SUs are served simultaneously via conjugate precoding at the P-APs/S-APs in the same time-frequency time-slot.

The secondary CCI inflicted at the PUs due to secondary concurrent transmissions in the same primary spectrum is mitigated by setting strict secondary transmit power constraints for the S-APs. Thus, the transmit power at each S-AP is constrained such that the total secondary CCI at any PU falls below the corresponding primary interference threshold. Then, the achievable rates of the PUs and SUs are derived in the presence of imperfectly estimated channel state information (CSI) with intra-system pilot contamination and estimation errors. Moreover, in order to guarantee user-fairness, an efficient transmit power control policy is designed for S-APs based on the max-min fairness criterion. Our analytical/numerical results are used to investigate the practical-viability of underlay spectrum-sharing in cell-free massive MIMO systems. We show that the distributed transmissions rendered by the cell-free massive MIMO can be used to boost the achievable rates of PUs/SUs in an underlay spectrum-sharing system set-up. Moreover, the proposed max-min fairness optimal transmit power control ensures uniform service to SUs by mitigating the near-far effect of downlink transmissions even with the mandatory secondary transmit power constraints at the S-APs.

II. System, channel and signal models

A. System and channel model

We consider a cell-free massive MIMO system with underlay spectrum-sharing (see Fig. 1). A primary system having M P-APs serves K single-antenna PUs by using its licensed spectrum. In order to enhance the overall spectrum efficiency by eliminating spectrum holes, a secondary system having N S-APs is underlaid. These N S-APs utilize the primary licensed spectrum to serve L single-antenna SUs. The secondary CCI inflicted at the PUs is mitigated by defining the secondary transmit power constraints for S-APs (see Section II-C). This ensures that the secondary CCI at the PUs falls below a predefined primary interference threshold such that the performance of the primary system is not hindered by the concurrent secondary transmissions in the same licensed primary spectrum. All P-APs and S-APs are connected to their respective primary/secondary central processing units (P-CPU/S-CPU). It is assumed that all P-APs/S-APs simultaneously serve all PUs/SUs in the same time-frequency resource block in a synchronized manner by adopting spatial multiplexing rendered by cell-free massive MIMO [3].

The channel between the mth P-AP and the kth PU is denoted by f_{mk}, where $k \in \{1, \cdots, K\}$ and $m \in \{1, \cdots, M\}$. The channel between the nth S-AP and the lth SU is denoted by g_{nl}, where $n \in \{1, \cdots, N\}$ and $l \in \{1, \cdots, L\}$. The interference channel between the nth S-AP and the kth PU is denoted by u_{nk}, while the interference channel between the mth P-AP and the lth SU is given by v_{ml}. These four channels can be modeled in a unified form as

$$h_{ab} = \tilde{h}_{ab}\zeta_{h_{ab}}^{1/2}, \tag{1}$$

where $h \in \{f, g, u, v\}$, $a \in \{m, n\}$ and $b \in \{k, l\}$. Here, $\tilde{h}_{ab} \sim \mathcal{CN}(0, 1)$ accounts for the small-scale Rayleigh fading, which is static during one coherence interval, while $\zeta_{h_{ab}}$ captures the large-scale fading, which is constant for several coherence intervals. In modeling $\zeta_{h_{ab}}$, it is assumed that PUs and SUs are spatially-distributed, and the corresponding long-term channel statistics are known a-prior at both P-APs/S-APs and PUs/SUs because they change very slowly. In fact, the estimation of these large-scale fading coefficients can be done in once about tens/hundreds of coherence intervals [13].

B. Uplink channel estimation

In practice, τ_p symbols out of the coherence interval having τ_c symbols are used for uplink channel estimation at the P-APs/S-APs. During this training period, all PUs and SUs send pilots towards the P-APs/S-APs. These pilot sequences are used to locally estimate the channels, f_{mk} and g_{nl}, at the P-APs and S-APs, respectively. It is worth noting that the channels corresponding to K/L PUs/SUs are estimated autonomously at each P-AP/S-AP in a decentralized manner. Thus, no cooperation/exchange of channel estimates among the P-APs and S-APs is required [3].

The number of orthogonal pilot sequences that can be allocated is a function of the channel coherence interval, i.e., the product of coherence time and coherence bandwidth, which is limited in practice [13]. Aimed at reducing the pilot overhead and hence to increase the number of served PUs/SUs in the same time-frequency resource block, pilot sequences must be shared among the primary/secondary systems. To this end, the following pilot sharing strategy is adopted.

We assumed that $Q \leq \min(K, L)$ number of pilot sequences is shared among the PUs and SUs. Thus, the pilots used by the PUs and SUs, $\mathbf{\Phi}_P$ and $\mathbf{\Phi}_S$, can be defined as

$$\mathbf{\Phi}_P = \left[\mathbf{\Phi}; \tilde{\mathbf{\Phi}}_P\right], \text{ and } \mathbf{\Phi}_S = \left[\mathbf{\Phi}; \tilde{\mathbf{\Phi}}_S\right], \tag{2}$$

where $\mathbf{\Phi} \in \mathbb{C}^{Q \times \tau_p}$ denotes the pilot sequence shared by Q PUs/SUs having a length of τ_p symbol durations. Furthermore, $\tilde{\mathbf{\Phi}}_P \in \mathbb{C}^{(K-Q)\times\tau_p}$ and $\tilde{\mathbf{\Phi}}_S \in \mathbb{C}^{(L-Q)\times\tau_p}$ are the pilot sequences assigned to the remaining $(K-Q)$ PUs and $(L-Q)$ SUs. The orthogonal property among these pilot sequences can be defined as $\mathbf{\Phi}\tilde{\mathbf{\Phi}}_P = \mathbf{0}$,

$\boldsymbol{\Phi}\tilde{\boldsymbol{\Phi}}_S = \mathbf{0}$ and $\tilde{\boldsymbol{\Phi}}_P\tilde{\boldsymbol{\Phi}}_S = \mathbf{0}$. For the sake of exposition, we define $\boldsymbol{\Phi}_P = \left[\boldsymbol{\phi}_{P_1}^T, \cdots, \boldsymbol{\phi}_{P_k}^T, \cdots, \boldsymbol{\phi}_{P_K}^T\right]^T$ and $\boldsymbol{\Phi}_S = \left[\boldsymbol{\phi}_{S_1}^T, \cdots, \boldsymbol{\phi}_{S_l}^T, \cdots \boldsymbol{\phi}_{S_L}^T\right]^T$, where $\|\boldsymbol{\phi}_{P_k}\|^2 = 1$ and $\|\boldsymbol{\phi}_{S_l}\|^2 = 1$ for $k \in \{1, \cdots, K\}$ and $l \in \{1, \cdots, L\}$. Thus, $\boldsymbol{\phi}_{P_k} \in \mathbb{C}^{1\times\tau_p}$ and $\boldsymbol{\phi}_{S_l} \in \mathbb{C}^{1\times\tau_p}$ are the pilot sequences sent by the kth PU and the lth SU, respectively.

The pilot signals received at the mth P-AP and the nth S-AP can be written as

$$\mathbf{y}'_{P_m} = \sqrt{\tau_p P}\sum_{k=1}^{K} f_{mk}\boldsymbol{\phi}_{P_k} + \sqrt{\tau_p P}\sum_{l=1}^{L} v_{ml}\boldsymbol{\phi}_{S_l} + \mathbf{w}_{P_m}, \quad (3a)$$

$$\mathbf{y}'_{S_n} = \sqrt{\tau_p P}\sum_{l=1}^{L} g_{nl}\boldsymbol{\phi}_{S_l} + \sqrt{\tau_p P}\sum_{k=1}^{K} u_{nk}\boldsymbol{\phi}_{P_k} + \mathbf{w}_{S_n}, \quad (3b)$$

where P is the average transmitted pilot power at each PU/SU. Moreover, $\mathbf{w}_{P_m}$ and $\mathbf{w}_{S_n}$ are additive white Gaussian noise (AWGN) vectors at the mth P-AP and the nth S-AP, respectively, having i.i.d. $\mathcal{CN}(0,1)$ elements.

By projecting (3a) and (3b) onto $\boldsymbol{\phi}_{P_k}$ and $\boldsymbol{\phi}_{S_l}$, respectively, sufficient statistics for estimating f_{mk} and g_{nl} can be given as

$$y_{P_{mk}} = \mathbf{y}'_{P_m}\boldsymbol{\phi}_{P_k}^H = \sqrt{\tau_p P}f_{mk} + \sqrt{\tau_p P}v_{mk} + \mathbf{w}_{P_m}\boldsymbol{\phi}_{P_k}^H, \quad (4a)$$

$$y_{S_{nl}} = \mathbf{y}'_{S_l}\boldsymbol{\phi}_{S_l}^H = \sqrt{\tau_p P}g_{nl} + \sqrt{\tau_p P}u_{nl} + \mathbf{w}_{S_n}\boldsymbol{\phi}_{S_l}^H. \quad (4b)$$

By using (4a) and (4b), the minimum mean square error (MMSE) channel estimates of f_{mk} and g_{nl} can be derived as (see Appendix A-A for derivation)

$$\hat{f}_{mk} = \frac{\mathbb{E}\left[y_{P_{mk}}^* f_{mk}\right]}{\mathbb{E}[|y_{P_{mk}}|^2]} y_{P_{mk}} = c_{P_{mk}} y_{P_{mk}}, \quad (5a)$$

$$\hat{g}_{nl} = \frac{\mathbb{E}\left[y_{S_{nl}}^* g_{nl}\right]}{\mathbb{E}[|y_{S_{nl}}|^2]} y_{S_{nl}} = c_{S_{nl}} y_{S_{nl}}, \quad (5b)$$

where $c_{P_{mk}}$ and $c_{S_{nl}}$ are given by

$$c_{P_{mk}} = \frac{\sqrt{\tau_p P}\zeta_{f_{mk}}}{\tau_p P\left(\zeta_{f_{mk}} + \zeta_{v_{mk}}\right) + 1}, \quad (6a)$$

$$c_{S_{nl}} = \frac{\sqrt{\tau_p P}\zeta_{g_{nl}}}{\tau_p P\left(\zeta_{g_{nl}} + \zeta_{u_{nl}}\right) + 1}. \quad (6b)$$

By exploiting TDD channel reciprocity, the P-APs and S-APs utilize locally estimated $\hat{f}_{mk}$ and $\hat{g}_{nl}$, respectively, as downlink channel estimates for constructing their precoders [13].

C. Secondary Transmit Power Constraints

In underlay spectrum-sharing, the transmit power at each S-AP must be constrained to guarantee that the secondary CCI inflicted at the PUs falls below the corresponding primary interference temperature of each PU. To this end, the total transmit power of the nth S-AP is defined as

$$P_{S_n} \triangleq \sum_{l=1}^{L} P_S \eta_{S_{nl}}, \quad (7)$$

where $n \in \{1, \cdots, N\}$, $l \in \{1, \cdots, L\}$ and $\sum_{l=1}^{L}\eta_{S_{nl}} \leq 1$. Moreover, $\eta_{S_{nl}}$ is the transmit power allocation coefficient at the nth S-AP for the lth SU, and P_S is the maximum allowable transmit power at each S-AP. In order to derive these secondary transmit power constraints, the CCI received at the kth PU from all S-APs can be written as

$$y_k = \sum_{n=1}^{N} u_{nk}x_{S_n} = \sqrt{P_S}\sum_{n=1}^{N}\sum_{l=1}^{L}\eta_{S_{nl}}^{1/2}u_{nk}\hat{g}_{nl}^* q_{S_l}, \quad (8)$$

where x_{S_n} is the transmit signal for the nth SU and defined in (13). Thus, the total average secondary CCI power (P_{I_k}) inflicted at the kth PU can be derived as

$$P_{I_k} = \mathbb{E}\left[|y_k|^2\right] = P_S \underbrace{\sum_{n=1}^{N}\sum_{l=1}^{L}\eta_{S_{nl}}\mathbb{E}\left[|u_{nk}\hat{g}_{nl}^*|^2\right]}_{Z_k}, \quad (9)$$

where Z_k is derived as (see Appendix A-B for derivation)

$$Z_k = \sum_{n=1}^{N}\eta_{S_{nk}}c_{S_{nk}}^2\zeta_{u_{nk}}\left(\tau_p P\left(\zeta_{g_{nk}} + 2\zeta_{u_{nk}}\right) + 1\right) + \sum_{n=1}^{N}\sum_{l\neq k}^{L}\eta_{S_{nl}}c_{S_{nl}}^2\zeta_{u_{nl}}\left(\tau_p P\left(\zeta_{g_{nl}} + \zeta_{u_{nl}}\right) + 1\right). \quad (10)$$

Then, the secondary transmit power constraint at the nth S-AP can be written as

$$P_{S_n} = \min\left(P_S, \frac{I_{T_1}}{Z_1}, \cdots, \frac{I_{T_k}}{Z_k}, \cdots, \frac{I_{T_K}}{Z_K}\right), \quad (11)$$

where I_{T_k} is the interference temperature of the kth PU. The power constraints in (11) will be used in our max-min transmit power control problem formulation in Section IV.

D. Signal model

Inspired by low computational complexity and near-optimal performance at large AP regime, the P-APs/S-APs adopt conjugate precoders, which are constructed via estimated channels, to transmit payload data towards the PUs/SUs. Thus, the transmitted signals by the mth P-AP and the nth S-AP can be written as

$$x_{P_m} = \sqrt{P_P}\sum_{k=1}^{K}\eta_{P_{mk}}^{1/2}\hat{f}_{mk}^* q_{P_k}, \quad (12)$$

$$x_{S_n} = \sqrt{P_S}\sum_{l=1}^{L}\eta_{S_{nl}}^{1/2}\hat{g}_{nl}^* q_{S_l}, \quad (13)$$

where q_{P_k} and q_{S_l} are the symbols intended for the kth PU and the lth SU, satisfying $\mathbb{E}\left[|q_{P_k}|^2\right] = 1$ and $\mathbb{E}\left[|q_{S_l}|^2\right] = 1$, respectively. In (12), $\eta_{P_{mk}}$ is the transmit power allocation coefficient at the mth P-AP and $\eta_{S_{nl}}$ is the transmit power allocation coefficient at the nth S-AP, and they are chosen to satisfy total power constraints.

The payload data signals received at the kth PU and the lth SU can be written as

$$r_{P_k} = \sum_{m=1}^{M} f_{mk}x_{P_m} + \sum_{n=1}^{N} u_{nk}x_{S_n} + w_{P_k}, \quad (14)$$

$$r_{S_l} = \sum_{n=1}^{N} g_{nl}x_{S_n} + \sum_{m=1}^{M} v_{ml}x_{P_m} + w_{S_l}, \quad (15)$$

where $w_{P_k} \sim \mathcal{CN}(0,1)$ and $w_{S_l} \sim \mathcal{CN}(0,1)$ are AWGN at the kth PU and the lth SU, respectively. Moreover, x_{P_m} and x_{S_n} are defined in (12) and (13), respectively.

III. Achievable Rate Analysis

A. Achievable rate analysis for the primary system

In TDD mode of operation, the uplink channels are estimated at the P-APs/S-APs via pilots sent by the PUs/SUs. In order to minimize the pilot/training overhead, no downlink pilots are transmitted for the purpose of downlink channel estimation at the PUs/SUs [13]. Moreover, the achievable rate gain that is attainable by sending downlink pilots has been

$$r_{P_k} = \underbrace{\sqrt{P_P}\mathbb{E}\left[\sum_{m=1}^{M}\eta_{P_{mk}}^{1/2} f_{mk}\hat{f}_{mk}^{*}\right] q_{P_k}}_{\text{desired signal}} + \underbrace{\sqrt{P_P}\left(\sum_{m=1}^{M}\eta_{P_{mk}}^{1/2} f_{mk}\hat{f}_{mk}^{*} - \mathbb{E}\left[\sum_{m=1}^{M}\eta_{P_{mk}}^{1/2} f_{mk}\hat{f}_{mk}^{*}\right]\right) q_{P_k}}_{\text{detection uncertainty}}$$
$$+ \underbrace{\sqrt{P_P}\sum_{i\neq k}^{K}\sum_{m=1}^{M}\eta_{P_{mi}}^{1/2} f_{mk}\hat{f}_{mi}^{*} q_{P_i}}_{\text{Inter-system interference caused by beamforminmg uncertainty}} + \underbrace{\sqrt{P_S}\sum_{j=1}^{L}\sum_{n=1}^{N}\eta_{S_{nj}}^{1/2} u_{nk}\hat{g}_{nj}^{*} q_{S_j}}_{\text{Inter-system interference caused by secondary CCI}} + \underbrace{w_{P_k}}_{\text{AWGN}} \tag{17}$$

shown to be negligibly small [14]. Thus, the PUs/SUs must relay on long-term/statistical downlink channel for signal decoding. This practice can be practically justified by virtue of channel hardening in massive MIMO [13].

By substituting (12) and (13) into (14), the received signal at the kth PU can be expanded as

$$r_{P_k} = \sqrt{P_P}\sum_{m=1}^{M}\eta_{P_{mk}}^{1/2} f_{mk}\hat{f}_{mk}^{*} q_{P_k} + \sqrt{P_P}\sum_{m=1}^{M}\sum_{i\neq k}^{K}\eta_{P_{mi}}^{1/2} f_{mk}\hat{f}_{mi}^{*} q_{P_i} + \sqrt{P_S}\sum_{n=1}^{N}\sum_{j=1}^{L}\eta_{S_{nj}}^{1/2} u_{nk}\hat{g}_{nj}^{*} q_{S_j} + w_{P_k}. \tag{16}$$

However, this received signal (16) must be re-arranged to decode with only statistical downlink channel knowledge at the PUs as (17) at the top of the page.

In (17), the desired signal and the effective noise, which consist of (i) interference caused by detection uncertainty, (ii) intra-system interference due to beamforming uncertainty, (iii) inter-system interference due to secondary CCI, and (iv) AWGN are uncorrelated. Inspired by the seminal massive MIMO literature [13], [14], the effective noise can be treated as the worst-case independently distributed Gaussian noise. Thus, the effective signal-to-interference-plus-noise ratio (SINR) pertaining to the kth PU can be written as

$$\gamma_{P_k} = \frac{P_P\left|\mathbb{E}\left[\sum_{m=1}^{M}\eta_{P_{mk}}^{1/2} f_{mk}\hat{f}_{mk}^{*}\right]\right|^2}{P_P\mathbb{V}\mathrm{ar}\left[\sum_{m=1}^{M}\eta_{P_{mk}}^{1/2} f_{mk}\hat{f}_{mk}^{*}\right] + \sum_{j=1}^{2} I_{Pj} + \mathbb{E}\left[|w_{P_k}|^2\right]}, \tag{18}$$

where I_{Pj} for $j \in \{1,2\}$ can be defined as

$$I_{P1} = P_P\mathbb{E}\left[\left|\sum_{i\neq k}^{K}\sum_{m=1}^{M}\eta_{P_{mi}}^{1/2} f_{mk}\hat{f}_{mi}^{*}\right|^2\right], \tag{19a}$$

$$I_{P2} = P_S\mathbb{E}\left[\left|\sum_{j=1}^{L}\sum_{n=1}^{N}\eta_{S_{nj}}^{1/2} u_{nk}\hat{g}_{nj}^{*}\right|^2\right]. \tag{19b}$$

The effective SINR in (18) can be computed in closed-form by evaluating the expectation and variance terms as (20) at the top of the next page (see Appendix B for the derivation). In (20), $\rho_{f_{mk}} = \sqrt{\tau_p P}\zeta_{f_{mk}} c_{P_{mk}}$ and the terms $\Psi_{I_{P_1}}(m,i)$, $\Psi_{I_{P_2}}(n,k)$ and $\Psi_{I_{P_2}}(n,j)$ are given by

$$\Psi_{I_{P_1}}(m,i) = \eta_{P_{mi}} c_{P_{mi}}^2 \zeta_{f_{mk}}\left[\tau_p P\left(\zeta_{f_{mi}} + \zeta_{v_{mi}}\right) + 1\right], \tag{21a}$$

$$\Psi_{I_{P_2}}(n,k) = \eta_{S_{nk}} c_{S_{nk}}^2 \zeta_{u_{nk}}\left[\tau_p P\left(\zeta_{g_{nk}} + 2\zeta_{u_{nk}}\right) + 1\right], \tag{21b}$$

$$\Psi_{I_{P_2}}(n,j) = \eta_{S_{nj}} c_{S_{nj}}^2 \zeta_{u_{nk}}\left[\tau_p P\left(\zeta_{g_{nj}} + \zeta_{u_{nj}}\right) + 1\right]. \tag{21c}$$

Then, the achievable rate of the kth PU can be defined as

$$R_{P_k} = \left(\frac{\tau_c - \tau_p}{\tau_c}\right)\log_2\left(1 + \gamma_{P_k}\right), \tag{22}$$

where the pre-log factor $((\tau_c - \tau_p)/\tau_c)$ captures the effective portion of coherence interval for payload data transmission, and γ_{P_k} is defined in (20).

B. Achievable rate definition for the secondary system

By following steps similar to (16)-(22), the achievable rate of the lth SU can be written as

$$R_{S_l} = \left(\frac{\tau_c - \tau_p}{\tau_c}\right)\log_2\left(1 + \gamma_{S_l}\right), \tag{23}$$

where the effective SINR of the lth SU can be defined as

$$\gamma_{S_l} = \frac{P_S\left|\mathbb{E}\left[\sum_{n=1}^{N}\eta_{S_{nl}}^{1/2} g_{nl}\hat{g}_{nl}^{*}\right]\right|^2}{P_S\mathbb{V}\mathrm{ar}\left[\sum_{n=1}^{N}\eta_{S_{nl}}^{1/2} g_{nl}\hat{g}_{nl}^{*}\right] + \sum_{j=1}^{2} I_{Sj} + \mathbb{E}\left[|w_{S_l}|^2\right]}, \tag{24}$$

where I_{Sj} for $j \in \{1,2\}$ can be defined as

$$I_{S_1} = P_S\mathbb{E}\left[\left|\sum_{j\neq l}^{L}\sum_{n=1}^{N}\eta_{S_{nj}}^{1/2} g_{nl}\hat{g}_{nj}^{*}\right|^2\right], \tag{25a}$$

$$I_{S_2} = P_P\mathbb{E}\left[\left|\sum_{i=1}^{K}\sum_{m=1}^{M}\eta_{P_{mi}}^{1/2} v_{ml}\hat{f}_{mi}^{*}\right|^2\right]. \tag{25b}$$

By following steps similar to those used for deriving (20), γ_{S_l} can be computed in closed-form as (26), where the terms $\Psi_{I_{S_1}}(n,j)$, $\Psi_{I_{S_2}}(m,l)$ and $\Psi_{I_{S_2}}(m,i)$ are given by

$$\Psi_{I_{S_1}}(n,j) = \eta_{S_{nj}} c_{S_{nj}}^2 \zeta_{g_{nl}}\left[\tau_p P\left(\zeta_{g_{nj}} + \zeta_{u_{nj}}\right) + 1\right], \tag{27a}$$

$$\Psi_{I_{S_2}}(m,l) = \eta_{P_{ml}} c_{P_{ml}}^2 \zeta_{v_{ml}}\left[\tau_p P\left(\zeta_{f_{ml}} + 2\zeta_{v_{ml}}\right) + 1\right], \tag{27b}$$

$$\Psi_{I_{S_2}}(m,i) = \eta_{P_{mi}} c_{P_{mi}}^2 \zeta_{v_{ml}}\left[\tau_p P\left(\zeta_{f_{mi}} + \zeta_{v_{mi}}\right) + 1\right]. \tag{27c}$$

IV. Transmit Power Control

Since the PUs/SUs are spatially-distributed, the achievable rates are affected by near-far effect. As such, in a uniform transmit power allocation scenario, the PUs/SUs having the strongest effective channels attain better rates, while the PUs/SUs with weaker channel conditions achieve considerably lower rates. This near-far effect is undesirable in providing a uniform quality-of-service across the cell-free system set-up, and hence, user-fairness must be guaranteed via optimal transmit power allocation for each P-AP/S-AP. Since the transmit power of each S-AP is further constrained by the secondary transmit power constraints in (11), the near-far effect will be more prominent for the secondary system. Thus, we primarily focused on transmit power control for the secondary system. To this end, a max-min transmit power control is proposed because it has been shown that such a scheme always be optimal in the sense of user-fairness in mitigating near-far effect.

$$\gamma_{P_k} = \frac{P_P \left(\sum\limits_{m=1}^{M} \eta_{P_{mk}}^{1/2} \rho_{f_{mk}} \right)^2}{P_P \sum\limits_{m=1}^{M} \eta_{P_{mk}} \rho_{f_{mk}} \zeta_{f_{mk}} + P_P \sum\limits_{i \neq k}^{K} \sum\limits_{m=1}^{M} \Psi_{I_{P_1}}(m,i) + P_S \sum\limits_{n=1}^{N} \Psi_{I_{P_2}}(n,k) + P_S \sum\limits_{j \neq k}^{L} \sum\limits_{n=1}^{N} \Psi_{I_{P_2}}(n,j) + 1} \tag{20}$$

$$\gamma_{S_l} = \frac{P_S \left(\sum\limits_{n=1}^{N} \eta_{S_{nl}}^{1/2} \rho_{g_{nl}} \right)^2}{P_S \sum\limits_{n=1}^{N} \eta_{S_{nl}} \rho_{g_{nl}} \zeta_{g_{nl}} + P_S \sum\limits_{j \neq l}^{L} \sum\limits_{n=1}^{N} \Psi_{I_{S_1}}(n,j) + P_P \sum\limits_{m=1}^{M} \Psi_{I_{S_2}}(m,l) + P_P \sum\limits_{i \neq l}^{K} \sum\limits_{m=1}^{M} \Psi_{I_{S_2}}(m,i) + 1} \tag{26}$$

By invoking the max-min transmit power control concepts [13], the power allocation coefficients of S-APs ($\eta_{S_{nl}}$ for $n \in \{1, \cdots, N\}$ and $l \in \{1, \cdots, L\}$) are computed to maximize the minimum achievable downlink rate among all SUs. Thus, the max-min transmit power control problem can be formulated as follows:

$$\max \min_{l \in \{1, \cdots, L\}} R_{S_l}, \tag{28a}$$

respect to $\eta_{S_{nl}}$, $l \in \{1, \cdots, L\}$ and $n \in \{1, \cdots, N\}$,

subject to $C_1 : \sum_{l=1}^{L} \eta_{S_{nl}} \rho_{g_{nl}} \leq 1, \qquad n \in \{1, \cdots, N\}, \tag{28b}$

$$C_2 : \eta_{S_{nl}} \geq 0, \ \ l \in \{1, \cdots, L\} \text{ and } n \in \{1, \cdots, N\}, \tag{28c}$$

$$C_3 : P_{S_n} \leq I_{T_k} / Z_k, \ \ k \in \{1, \cdots, K\}, \tag{28d}$$

where R_{S_l} is defined in (23). Moreover, C_1 is obtained by invoking the maximum allowable transmit power (P_S) constraint pertaining to the transmit signal (x_{S_n}) at the nth S-AP as follows:

$$P_{S_n} = \mathbb{E}\left[|x_{S_n}|^2\right] \leq P_S \ \Rightarrow \ \mathbb{E}\left[\left| \sqrt{P_S} \sum_{l=1}^{L} \eta_{S_{nl}}^{1/2} \hat{g}_{nl}^* q_{S_l} \right|^2 \right] \leq P_S,$$

$$\sum_{l=1}^{L} \eta_{S_{nl}} \mathbb{E}[|\hat{g}_{nl}^* q_{S_l}]\,|^2 \leq 1 \ \ \Rightarrow \ \ \sum_{l=1}^{L} \eta_{S_{nl}} \rho_{g_{nl}} \leq 1, \tag{29}$$

where $\rho_{g_{nl}}$ is defined as $\rho_{g_{nl}} \triangleq \mathbb{E}\left[|\hat{g}_{nl}^* q_{S_l}|^2\right] = \mathbb{E}\left[|\hat{g}_{nl}|^2\right] = \sqrt{\tau_p P} \zeta_{g_{nl}} c_{S_{nl}}$. Furthermore, C_3 is obtained by adopting the secondary transmit power constraints in (11).

Since R_{S_l} in (28) is a monotonically increasing function of γ_{S_l} in (26), R_{S_l} can equivalently be replaced γ_{S_l}. In a max-min algorithm, a common SINR can be set to all SUs and then, the transmit power can be allocated to S-APs such that this common SINR is maximized. To this end, by introducing a common SINR denoted by λ for all SUs such that $\min_{l \in \{1, \cdots, L\}} \gamma_{S_l} \geq \lambda$ and by defining a slack variable $\mu_{S_{nl}} \triangleq \eta_{S_{nl}}^{1/2}$, we can equivalently reformulate (28) as

$$\max \min_{l \in \{1, \cdots, L\}} \lambda, \tag{30a}$$

respect to $\mu_{S_{nl}}$, $l \in \{1, \cdots, L\}$ and $n \in \{1, \cdots, N\}$,

subject to

$$\frac{1}{\lambda} \left(\sum_{n=1}^{N} \mu_{S_{nl}} \rho_{g_{nl}} \right)^2 \geq \sum_{n,j=1}^{N,L} \mu_{S_{nl}}^2 a_{nl} + \frac{P_P}{P_S} \sum_{m,i=1}^{M,K} b_{mk} + \frac{1}{P_S}, \tag{30b}$$

$$C_1 : \sum_{l=1}^{L} \mu_{S_{nl}}^2 \rho_{g_{nl}} \leq 1, \qquad n \in \{1, \cdots, N\}, \tag{30c}$$

$$C_2 : \mu_{S_{nl}} \geq 0, \ \ l \in \{1, \cdots, L\} \text{ and } n \in \{1, \cdots, N\}, \tag{30d}$$

$$C_3 : P_{S_n} \leq I_{T_k} / Z_k, \ \ k \in \{1, \cdots, K\}, \tag{30e}$$

where a_{nl} and b_{mk} in (30b) are given by

$$a_{nl} = \begin{cases} \rho_{g_{nl}} \zeta_{g_{nl}}, & \text{if} \quad j = l, \\ \Psi_{I_{S_1}}(n,j), & \text{otherwise}, \end{cases} \tag{31a}$$

$$b_{mk} = \begin{cases} \Psi_{I_{S_2}}(m,l), & \text{if} \quad i = l, \\ \Psi_{I_{S_2}}(m,i), & \text{otherwise}. \end{cases} \tag{31b}$$

In (30b), the equality holds at the optimum solution.

The objective function in (30) is quasi-concave, and the optimization problem is quasi-concave [3]. Thus, an optimal solution based on Bisection method is proposed as follows:

1) Define an initial region for the objective function by selecting λ_{min} and λ_{max} values. Choose a tolerance $\epsilon > 0$.
2) Calculate $\lambda = (\lambda_{max} + \lambda_{min})/2$ and solve the convex feasibility problem, which can be given as

$$\|\boldsymbol{V}_{S_l}\| \leq \frac{1}{\sqrt{\lambda}} \left(\sum_{n=1}^{N} \mu_{S_{nl}} \rho_{g_{nl}} \right), l \in \{1, \cdots, L\}, \tag{32}$$

which is subjected to C_1, C_2 and C_3. Moreover, $\boldsymbol{V}_{S_l} \triangleq \left[\mathbf{v}_{S_{l1}}^T \ \mathbf{v}_{S_{l2}}^T \ 1/P_S\right]^T$, where

$$\mathbf{v}_{S_{L1}} \triangleq [\mu_{S_{n1}} \sqrt{a_{n1}}, \cdots, \mu_{S_{nL}} \sqrt{a_{nL}}\,]^T, \tag{33a}$$

$$\mathbf{v}_{S_{l2}} \triangleq \left[\sqrt{b_{m1}}, \cdots, \sqrt{b_{mK}}\right]^T. \tag{33b}$$

3) Then, according to the status of the problem, we have

$$\lambda = \begin{cases} \lambda_{min}, & \text{if feasible}, \\ \lambda_{max}, & \text{otherwise}. \end{cases} \tag{34}$$

4) Stop if $\lambda_{max} - \lambda_{min} < \epsilon$. Otherwise go to Step 2.

A max-min transmit power control problem for the primary system can also be formulated by following steps similar to those in (28a)-(28d). However, this problem formulation is omitted for the sake of brevity. In the case with uniform power allocation, the coefficients $\eta_{P_{mk}}$ are computed as

$$\mathbb{E}\left[\left| \sqrt{P_P} \sum_{k=1}^{K} \eta_{P_{mk}}^{1/2} \hat{f}_{mk}^* q_{P_k} \right|^2 \right] = P_P,$$

$$\sum_{k=1}^{K} \eta_{P_{mk}} \mathbb{E}\left[\left| \hat{f}_{mk}^* q_{P_k} \right|^2 \right] = 1,$$

$$\eta_{P_{mk}} = \frac{1}{\sum_{k=1}^{K} \rho_{f_{mk}}}, \quad \text{for} \quad k \in \{1, \cdots, K\}, \tag{35}$$

where $\rho_{f_{mk}}$ is given by $\rho_{f_{mk}} \triangleq \mathbb{E}\left[|\hat{f}_{mk}^* q_{P_k}|^2\right] = \mathbb{E}\left[|\hat{f}_{mk}|^2\right] = \sqrt{\tau_p P} \zeta_{f_{mk}} c_{P_{mk}}$.

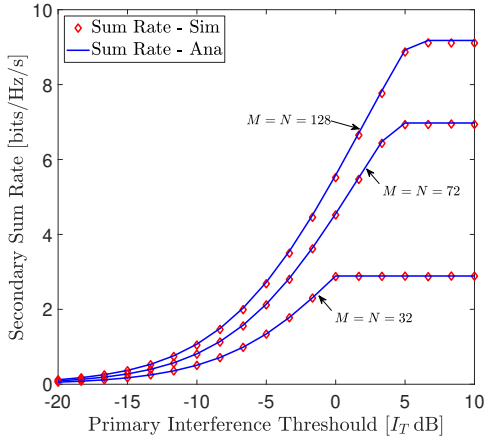

Fig. 2. Secondary sum rate versus the primary interference threshold (I_T) for $K = L = 4$, $\sigma_P^2 = \sigma_S^2 = 1$, $\nu = 2.4$, $d_0 = 1$ m.

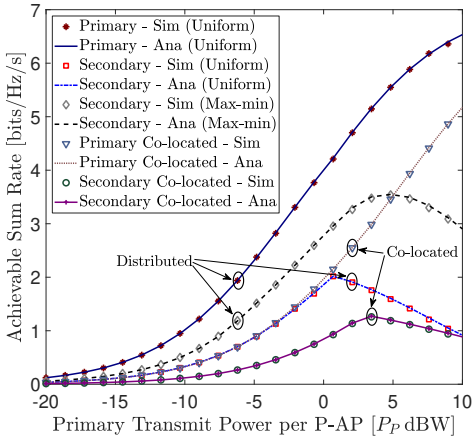

Fig. 3. Achievable sum rate versus primary transmit power for $M = N = 32$, $K = L = 4$, $I_T = 0$ dB, $\sigma_P^2 = \sigma_S^2 = 1$, $\nu = 2.4$, and $d_0 = 1$ m.

V. Numerical Results

Simulation parameters are as follows: $\tau_c = 196$, $\tau_p = \max(K, L)$ and $\zeta_{h_{ab}} = (d_0/d_{ab})^{\nu} \times 10^{\varphi_{ab}/10}$, where d_{ab} is a transmission distance, d_0 is a reference distance, and ν is path-loss exponent, and $10^{\varphi_{ab}/10}$ captures the shadow fading with $\varphi_{ab} \sim \mathcal{N}(0, 8)$. The P-APs/S-APs are uniformly distributed, while PUs/SUs are randomly distributed over an area of $800 \times 800\,\mathrm{m}^2$.

In Fig. 2, the achievable secondary sum rate is plotted as a function of the primary interference temperature (I_T). The simulation curves are plotted via Monte-Carlo simulations by using (11), and the analytical curves are plotted by using (23). Three sets of sum rate curves are plotted by varying the number of P-APs and S-APs as $M = N = 32$, $M = N = 72$ and $M = N = 128$. The secondary sum rate grows exponentially with I_T in the low I_T regime, while it saturates to a constant maximum in the high I_T regime. The maximum saturation depends heavily on N. The reason for this behavior is as follows: In the low I_T regime, the PUs can withstand only to very small level of secondary CCI, and hence, the primary system is strictly protected against detrimental impacts of secondary underly spectrum-sharing. Thus, the secondary transmit power constants at the S-APs are more stringent, and the corresponding low secondary transmit powers result in smaller secondary achievable rates. However, as I_T grows large, the secondary system is allowed to inflict a higher amount of secondary CCI at the PUs. This in turn allows S-APs to transmit at higher transmit power levels than in low I_T regime. Consequently, the achievable secondary sum rate increases when I_T grows large. However, the secondary sum rate saturates to a maximum once the secondary power constraints in (11) are met. At this operating point, the S-APs utilize their maximum allowable transmit power P_S, and consequently, the secondary sum rate becomes independent of I_T. Therefore, the secondary sum rate saturates a constant, which is the maximum achievable sum rate limit by utilizing the maximum allowable transmit power of P_S at the S-APs.

In Fig. 3, the achievable sum rates of the primary and secondary systems are plotted as a function of the transmit power per P-AP (P_P). The maximum allowable transmit power (P_S) at each S-AP is kept at $P_P/2$. Then, the secondary transmit power coefficients are computed via the proposed max-min power algorithm in Section IV, and the resulting sum rate is compared against that of the uniform power allocation. Fig. 3 depicts that the primary sum rate increases monotonically with the unconstrained P_P. However, in max-min power allocation, the secondary sum rate first increases gradually up to a maximum in the low P_P regime, and then it decreases as P_P increases without bound. The reason for this behavior can be described as follows: When the secondary sum rate reaches a maximum, the S-APs transmit with their maximum allowable transmit power P_S. In the meantime, the transmit powers at the P-APs keep growing and this in turn inflicts a higher level of primary CCI at the SUs. Consequently, the secondary sum rate gradually decreases as P_P grows large without bound. On the contrary, when it comes to uniform power allocation for the secondary system, its achievable sum rate decays gradually with increasing P_P. Thus, Fig. 3 clearly reveals that the proposed max-min power allocation significantly outperforms the uniform power allocation. In Fig. 3, performance of the proposed cell-free massive MIMO with underlay spectrum-sharing is also compared with a co-located counterpart, and our results reveal that the former outperforms the latter in terms of the achievable sum rate.

VI. Conclusion

The coexistence of underlay spectrum-sharing and cell-free massive MIMO has been explored by deriving the achievable rates for both primary and secondary systems. A max-min fairness optimal transmit power control has been proposed for the S-APs, while satisfying the secondary transmit power constraints subject to primary interference temperature. Our analysis reveals that the achievable rates of both primary and secondary systems can be boosted by imposing carefully-designed secondary transmit power constraints at each distributed S-AP. Moreover, we conclude that max-min transmit power control at the S-APs can significantly boost the achievable sum rate over the uniform power allocation. Thus, a secondary system can be operated in the same licensed spectrum without hindering the performance of the primary system operated in a cell-free arrangement.

APPENDIX A

A. Derivation of the MMSE estimate

By substituting (4a) into (5a), $\hat{f}_{mk}$ can be derived as [15]

$$\begin{aligned}\hat{f}_{mk} &= \frac{\mathbb{E}\left[\left(\sqrt{\tau_p P} f^*_{mk} + \sqrt{\tau_p P} v^*_{mk} + \tilde{w}^*_{P_m}\right) f_{mk}\right]}{\mathbb{E}\left[\left|\sqrt{\tau_p P} f_{mk} + \sqrt{\tau_p P} v_{mk} + \tilde{w}_{P_m}\right|^2\right]} y_{P_{mk}}, \\ &= \frac{\sqrt{\tau_p P}\mathbb{E}[f^*_{mk} f_{mk}]}{\tau_p P \mathbb{E}[|f_{mk}|^2] + \tau_p P \mathbb{E}[|v_{mk}|^2] + \mathbb{E}[|\tilde{w}_{P_m}|^2]} y_{P_{mk}}, \\ &= c_{P_{mk}} y_{P_{mk}}, \end{aligned} \tag{36}$$

where $c_{P_{mk}}$ is defined in (6a), and $\tilde{w}_{P_m} = \mathbf{w}_{P_m} \boldsymbol{\phi}^H_{P_k}$. Similarly, the MMSE estimate of g_{nl} can be derived as (5b).

B. Derivation of Z_k in (10)

By substituting (5b) and (4b) into (9), Z_k is computed as

$$\begin{aligned} Z_k =& \sum_{n=1}^{N} \eta_{S_{nk}} c^2_{S_{nk}} \mathbb{E}\left[\left| u_{nk} \left(\sqrt{\tau_p P} g_{nk} + \sqrt{\tau_p P} u_{nk} + \mathbf{w}_{S_n} \boldsymbol{\phi}^H_{S_k}\right)^* \right|^2\right] \\ &+ \sum_{n=1, l\neq k}^{N, L} \eta_{S_{nl}} c^2_{S_{nl}} \mathbb{E}\left[\left| u_{nk} \left(\sqrt{\tau_p P} g_{nl} + \sqrt{\tau_p P} u_{nl} + \mathbf{w}_{S_n} \boldsymbol{\phi}^H_{S_l}\right)^* \right|^2\right], \\ &= \sum_{n=1}^{N} \eta_{S_{nk}} c^2_{S_{nk}} \zeta_{u_{nk}} \left(\tau_p P \left(\zeta_{g_{nk}} + 2\zeta_{u_{nk}}\right) + 1\right) \\ &+ \sum_{n=1}^{N} \sum_{l\neq k}^{L} \eta_{S_{nl}} c^2_{S_{nl}} \zeta_{u_{nk}} \left(\tau_p P \left(\zeta_{g_{nl}} + \zeta_{u_{nl}}\right) + 1\right). \end{aligned} \tag{37}$$

APPENDIX B
DERIVATION OF SINR IN (18)

The expectation in numerator of (18) can be derived as

$$\begin{aligned} \mathbb{E}\left[\sum_{m=1}^{M} \eta^{1/2}_{P_{mk}} f_{mk} \hat{f}^*_{mk}\right] &= \sum_{m=1}^{M} \eta^{1/2}_{P_{mk}} \mathbb{E}\left[\left(\hat{f}_{mk} + \epsilon_{f_{mk}}\right) f^*_{mk}\right], \\ &= \sum_{m=1}^{M} \eta^{1/2}_{P_{mk}} \mathbb{E}\left[\hat{f}_{mk} f^*_{mk}\right] \overset{(a)}{=} \sum_{m=1}^{M} \eta^{1/2}_{P_{mk}} \rho_{f_{mk}}, \end{aligned} \tag{38}$$

where $\epsilon_{f_{mk}}$ is an error of f_{mk} such that $f_{mk} = \hat{f}_{mk} + \epsilon_{f_{mk}}$, satisfying $\mathbb{E}[\epsilon_{f_{mk}} f^*_{mk}] = 0$. In (38), the step (a) is written by substituting (5a) and then evaluating expectation term as

$$\mathbb{E}\left[|\hat{f}_{mk}|^2\right] = c^2_{P_{mk}} \mathbb{E}\left[|y_{P_{mk}}|^2\right] = \sqrt{\tau_p P} \zeta_{f_{mk}} c_{P_{mk}} = \rho_{f_{mk}}. \tag{39}$$

Then, the variance term in (18) can be derived as

$$\begin{aligned} &\mathbb{V}\mathrm{ar}\left[\sum_{m=1}^{M} \eta^{1/2}_{P_{mk}} f_{mk} \hat{f}^*_{mk}\right] \\ &= \sum_{m=1}^{M} \eta_{P_{mk}} \left(\mathbb{E}\left[\left|\left(\hat{f}_{mk} + \epsilon_{f_{mk}}\right) \hat{f}^*_{mk}\right|^2\right] - \rho^2_{f_{mk}}\right), \\ &= \sum_{m=1}^{M} \eta_{P_{mk}} \left(2\rho^2_{f_{mk}} + \rho_{f_{mk}} \left(\zeta_{f_{mk}} - \rho_{f_{mk}}\right) - \rho^2_{f_{mk}}\right), \\ &= \sum_{m=1}^{M} \eta_{P_{mk}} \rho_{f_{mk}} \zeta_{f_{mk}}. \end{aligned} \tag{40}$$

The expectation in (19a) can be compute as

$$\begin{aligned} &\mathbb{E}\left[\left|\sum_{i\neq k}^{K} \sum_{m=1}^{M} \eta^{1/2}_{P_{mi}} f_{mk} \hat{f}^*_{mi}\right|^2\right] \\ &\overset{(b)}{=} \sum_{i\neq k}^{K} \sum_{m=1}^{M} \mathbb{E}\left[\left|\eta^{1/2}_{P_{mi}} f_{mk} c_{P_{mi}} y_{P_{mi}}\right|^2\right], \\ &\overset{(c)}{=} \tau_p P \sum_{i\neq k}^{K} \sum_{m=1}^{M} \eta_{P_{mi}} c^2_{P_{mi}} \zeta_{f_{mk}} \left(\zeta_{f_{mi}} + \zeta_{v_{mi}}\right) \\ &+ \tau_p P \sum_{i\neq k}^{K} \sum_{m=1}^{M} \eta_{P_{mi}} c^2_{P_{mi}} \zeta_{f_{mk}}. \end{aligned} \tag{41}$$

where the steps (b) and (c) are written by using (5a) and (4a), respectively. The expectation term in (19b) can be derived by following steps similar to those used in (37) as follows:

$$\begin{aligned} &\mathbb{E}\left[\left|\sum_{j=1}^{L} \sum_{n=1}^{N} \eta^{1/2}_{S_{nj}} u_{nk} \hat{g}^*_{nj}\right|^2\right] \\ &= \sum_{n=1}^{N} \eta_{S_{nk}} c^2_{S_{nk}} \zeta_{u_{nk}} \left(\tau_p P \left(\zeta_{g_{nk}} + 2\zeta_{u_{nk}}\right) + 1\right) \\ &+ \sum_{j\neq k}^{L} \sum_{n=1}^{N} \eta_{S_{nj}} c^2_{S_{nj}} \zeta_{u_{nk}} \left(\tau_p P \left(\zeta_{g_{nj}} + \zeta_{u_{nj}}\right) + 1\right). \end{aligned} \tag{42}$$

By substituting (38), (40), (41) and (42) into (18), the desired SINR can be derived as in (20).

REFERENCES

[1] E. G. Larsson, O. Edfors, F. Tufvesson, and T. L. Marzetta, "Massive MIMO for next generation wireless systems," *IEEE Commun. Mag.*, vol. 52, no. 2, pp. 186–195, Feb. 2014.

[2] H. Q. Ngo *et al.*, "Cell-free massive MIMO: Uniformly great service for everyone," in *Proc. IEEE 16th Int. Workshop on Signal Process. Advances in Wireless Commun. (SPAWC)*, June 2015, pp. 201–205.

[3] ——, "Cell-free massive MIMO versus small cells," *IEEE Trans. Wireless Commun.*, vol. 16, no. 3, pp. 1834–1850, Mar. 2017.

[4] E. Nayebi *et al.*, "Precoding and power optimization in cell-free massive MIMO systems," *IEEE Transactions on Wireless Communications*, vol. 16, no. 7, pp. 4445–4459, July 2017.

[5] T. C. Mai, H. Q. Ngo, M. Egan, and T. Q. Duong, "Pilot power control for cell-free massive MIMO," *IEEE Transactions on Vehicular Technology*, pp. 1–1, 2018.

[6] A. Goldsmith, S. A. Jafar, I. Maric, and S. Srinivasa, "Breaking spectrum gridlock with cognitive radios: An information theoretic perspective," *Proc. IEEE*, vol. 97, no. 5, pp. 894–914, May 2009.

[7] L. Wang *et al.*, "Massive MIMO in spectrum sharing networks: Achievable rate and power efficiency," *IEEE Systems Journal*, vol. 11, no. 1, pp. 20–31, March 2017.

[8] H. Al-Hraishawi, G. A. A. Baduge, H. Q. Ngo, and E. G. Larsson, "Multi-cell massive MIMO uplink with underlay spectrum sharing," *IEEE Transactions on Cognitive Communications and Networking*, 2018, accepted.

[9] Y. Li, D. Kudathanthirige, and G. A. A. Baduge, "Massive MIMO relay networks with underlay spectrum sharing," *IEEE Trans. Cog. Commun. Netw.*, Oct. 2017, accepted.

[10] S. J. Silva, M. Ardakani, and C. Tellambura, "Relay Selection for Cognitive Massive MIMO Two-Way Relay Networks," in *IEEE Wireless Commun. and Netw. Conf. (WCNC)*, San Francisco, CA, USA, Mar. 2017, pp. 1–6.

[11] S. Kusaladharma and C. Tellambura, "Massive MIMO based underlay networks with power control," in *Proc. IEEE Int. Conf. on Commun. (ICC)*, May 2016, pp. 1–6.

[12] ——, "Secondary user interference characterization for spatially random underlay networks with massive MIMO and power control," *IEEE Trans. Veh. Technol.*, vol. 66, no. 9, pp. 7897–7912, Sep. 2017.

[13] T. L. Marzetta, E. G. Larsson, H. Yang, and H. Q. Ngo, *Fundamentals of Massive MIMO*. Cambridge University Press, Cambridge, UK, 2016.

[14] H. Q. Ngo and E. G. Larsson, "No Downlink Pilots Are Needed in TDD Massive MIMO," *IEEE Trans. Wireless Commun.*, vol. 16, no. 5, pp. 2921–2935, May 2017.

[15] S. M. Kay, *Fundamentals of Statistical Signal Processing: Estimation Theory*. Englewood Cliffs, NJ: Prentice Hall, 1993.